SUPPLEMENTARY INFORMATION FOR

Spatial Localization of Bacteria Controls Coagulation of Human Blood by "Quorum Acting"

Christian J. Kastrup[1], James Q. Boedicker[1], Andrei P. Pomerantsev[2], Mahtab Moayeri[2], Yao Bian[3], Rebecca R. Pompano[1], Timothy R. Kline[1], Patricia Sylvestre[4], Feng Shen[1], Stephen H. Leppla[2], Wei-Jen Tang[3], and Rustem F. Ismagilov[1]*

[1]Department of Chemistry and Institute for Biophysical Dynamics, The University of Chicago, 929 East 57th Street, Chicago, Illinois 60637

[2]Bacterial Toxins and Therapeutics Section, National Institute of Allergy and Infectious Diseases, National Institutes of Health, 30 Convent Dr., Building 30, Room 303 Bethesda, Maryland 20892-4349

[3]Ben-May Institute for Cancer Research, The University of Chicago, 929 East 57th Street, Chicago, Illinois 60637

[4]Institut Pasteur, Unité des Toxines et Pathogénie Bactérienne, Paris F-75015, France, and CNRS, URA 2172, Paris F-75015, France

SUPPLEMENTARY FIGURES
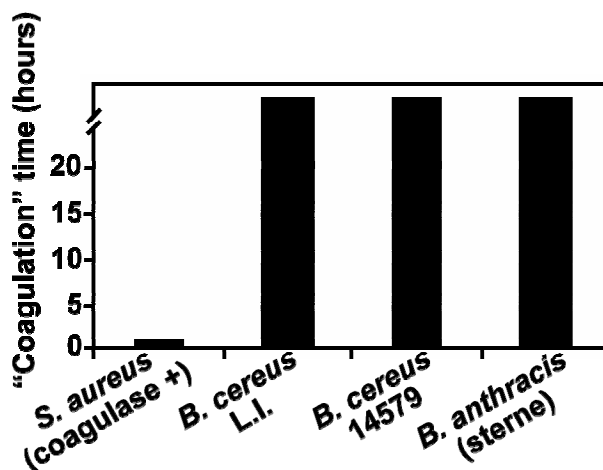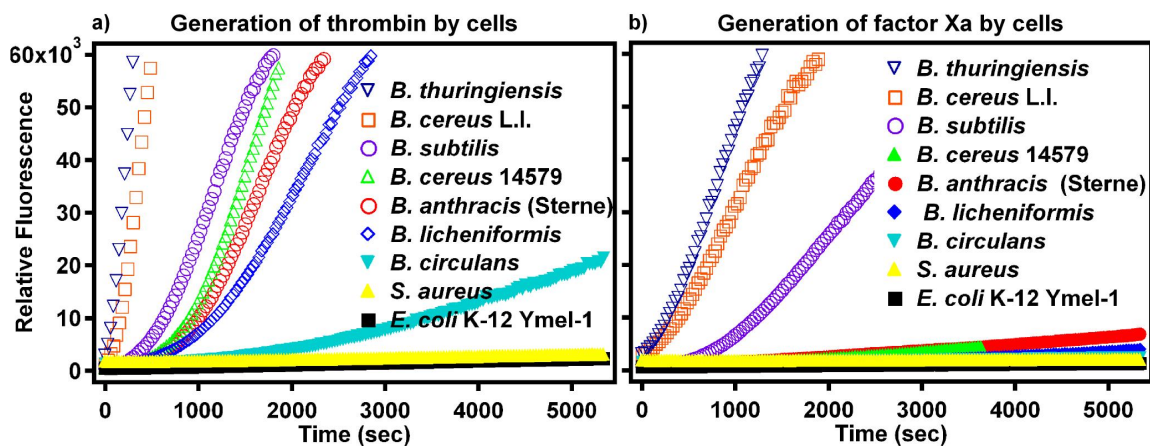

Figure S1. *B. cereus* and *B. anthracis* do not give a positive result for the "coagulase test", which measures production of fibrin in Ca^{2+}-deficient rabbit plasma, while *S. aureus* (control strain) gives a positive result. The break in the Y-axis indicates that the experiment was terminated at 26 h. No fibrin was observed for *B. cereus* or *B. anthracis* during that time.
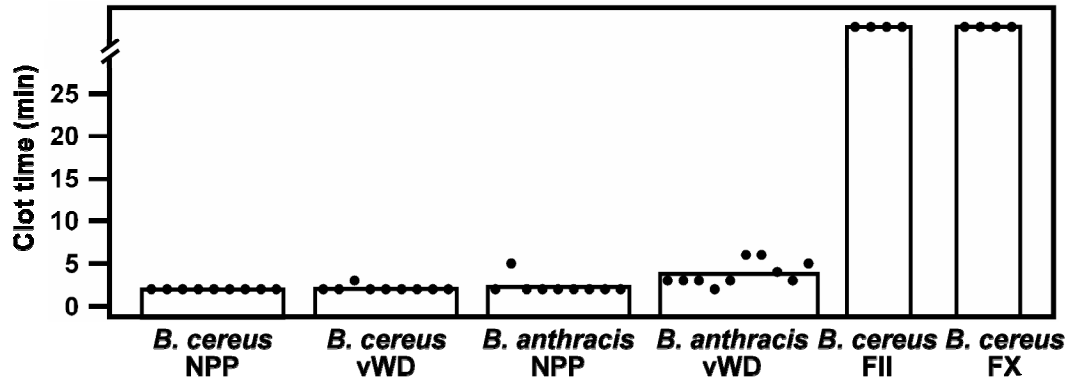
Figure S2. *B. cereus* and *B. anthracis* rapidly initiated coagulation of plasma deficient in von Willebrand factor and platelets, but not plasma deficient in prothrombin or factor X. Graph shows the clot times of platelet poor plasma from a donor with severe trait von Willebrand disease (vWD), the clot times of normal pooled platelet-poor plasma (NPP), and the clot times of plasma depleted in prothrombin (FII) and factor X (FX) (which did not initiate clotting within 30 min).
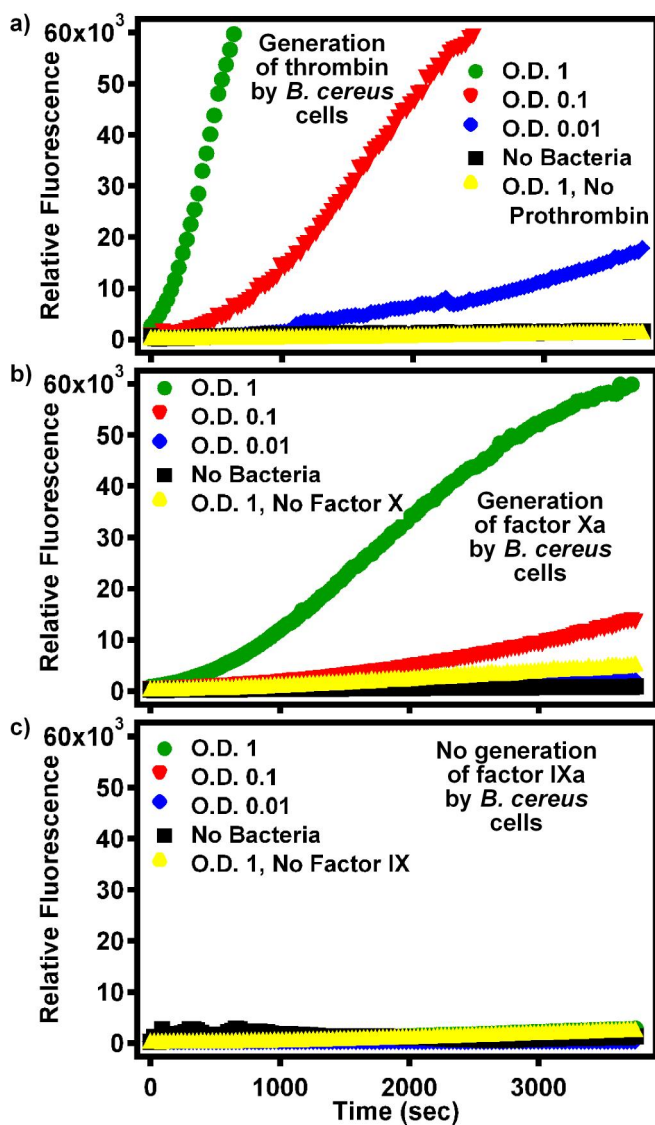
Figure S3. *B. cereus* cells directly activate factor X and prothrombin. (a-c) Graphs quantifying the activation of coagulation factors prothrombin (a), factor X (b), and factor IX (c) by bacteria. In these experiments, solutions contained only bacteria, the purified coagulation factor, and a fluorescent substrate for that factor.

a) Generation of thrombin by cells

b) Generation of factor Xa by cells

Legend:
- ▽ *B. thuringiensis*
- ☐ *B. cereus* L.l.
- ○ *B. subtilis*
- △ *B. cereus* 14579
- ○ *B. anthracis* (Sterne)
- ◇ *B. licheniformis*
- ▼ *B. circulans*
- ▲ *S. aureus*
- ■ *E. coli* K-12 Ymel-1

Figure S4. Bacterial cells from several *Bacillus* species activate prothrombin (a) and factor X (b) while control species of *E. coli* and *S. aureus* do not. In these experiments, solutions contained only bacteria, the purified coagulation factor, and a fluorescent substrate for that factor.
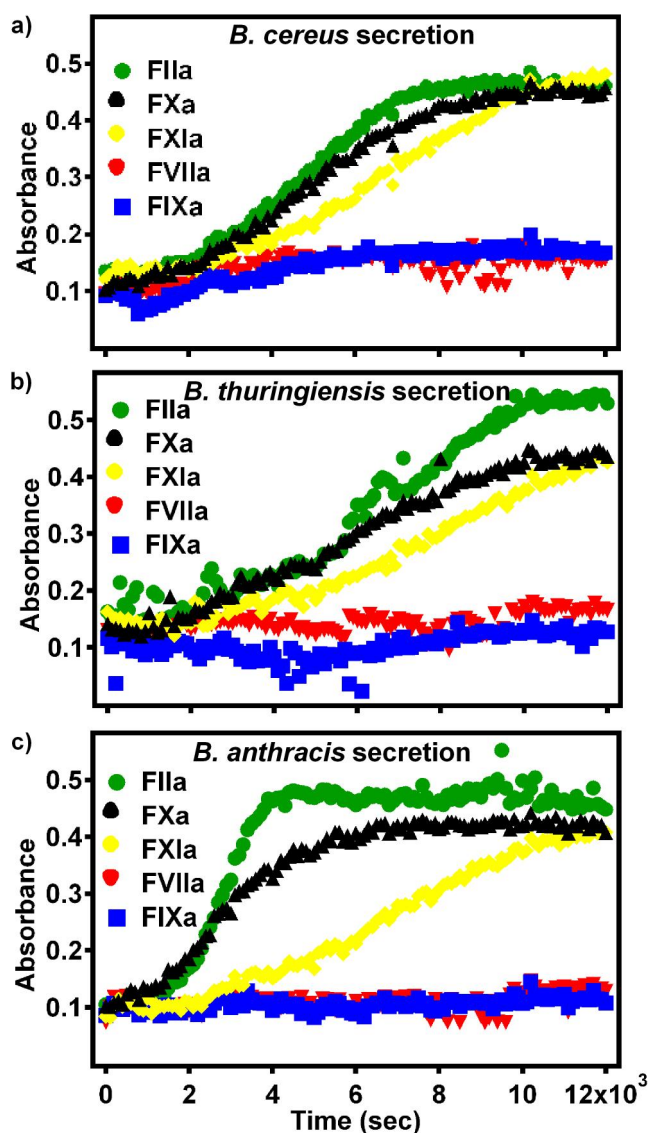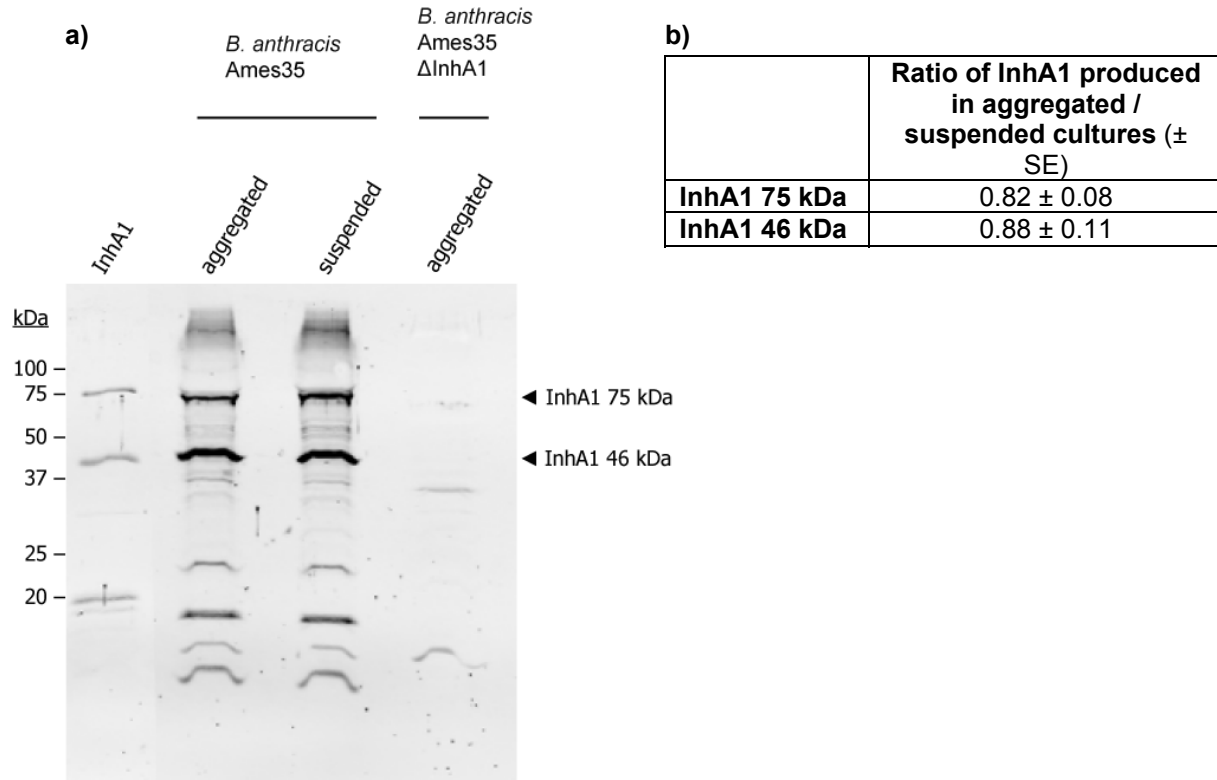
Figure S5. Secreted components from *B. cereus*, *B. thuringiensis*, and *B. anthracis* A35 directly activate prothrombin, factor X, and factor XI, but not factor VII or Factor IX. (a-c) Graphs quantifying the activation of coagulation factors by *B. cereus* (a), *B. thuringiensis* (b), and *B. anthracis* (c). In these experiments, bacterial cells were removed from the solutions, leaving the secreted components behind. The absorbance of these solutions was measured after the purified coagulation factor, and a chromogenic substrate for that factor were added. The curves shown indicate the absorbance values after the curves from two control experiments, i) without secreted components and ii) without the coagulation factor, were subtracted.

**MNKKPFKVLSSIALTAVLGLSFGAGGQSVYAETPVNKTATSPVDDHLIPEERLADALKKRGVIDSKASE
KETKKAVEKYVENKKGENPGKEVTNGDPLTKEASDFVKKVKDAKADTKEKLDKPATGTPAATGPVRGGL
NGKVPTSPAKQKAYNGDVRKDKVLVLLVEYADFKHNNIDKEPGYMYSEDFNKEHYEKMLFGDEPFTLDD
GSKIETFKQYYEEQSGGSYTVDGTVTKWLTVPGKAADYGADAATGHDNKGPKGPRDLVKDALKAAVDSG
LDLSEFDQFDQYDVNGDGNKNQPDGLIDHLMIIHAGVGQEAGGGKLGDDAIWSHRWTVGPKPFPIEGTQ
AKVPYW<u>GGK</u>**MAAFDYTIEPEDGAVGVFA**HEYGH**DLGLPDEYDTQYSGHGEPVQAWSIMSGGSWAGKIAG
TTPTSFSPQNKEFFQKTIGGNWANIVEVDYEKLNKGIGLATYLDQSVTKTNRPGMIRVNLPDKDIKTID
PAFGKQYYYSTKGDDLHTKLETPLFDLTNATTAKFDFKSLYEIEAEYDFLEVHAVTEDGQQTLIERLGE
KANNGNADSTNGKWIDKSYDLSQFKGKKVKLTFDYITDGGLALNGFLLDNASLTVDGKVVFSDDAEGTP
QFKLDGFAVSNGTEKKSHNYYVEWRNYAGSDNALKFARGPEYNTGMVVWYADSAYTDNWVGVHPGHGFL
GVVDSHPEAIVGTLNGKPTVESSTRFQIADAAFSFDKTPAWKVVSPTRGTYTYNGLAGVPKFDDSKTYI
NQQIPDAGRILPNLGLKFEVVGQADDNSAGAVRLYR

Figure S6. Inactivation of InhA1. The InhA1 protease (BA1295) was inactivated by using a procedure previously described for other *B. anthracis* genes[3]. This resulted in the insertion of the 34-base pair LoxP sequence into the middle of the gene. The sequence of original InhA1 (BA1295) protease is shown. DNA sequencing of the mutated strain chromosomal DNA confirmed that the LoxP sequence was inserted at the location corresponding to the GGK sequence (underlined). The resulting frame shift leads to truncation of the protein, which then is predicted to contain the sequence shown in bold followed by 13 out-of-frame (non-sense) residues (not shown). Thus, the truncated protein lacks the active site, zinc-binding region shown in red and the rest of the native sequence.
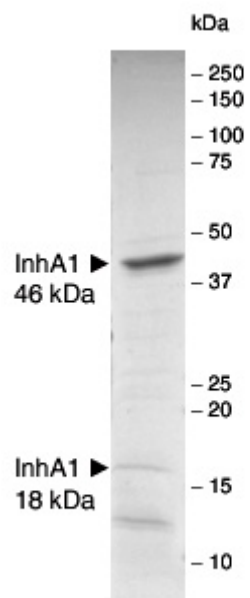
Figure S7. Purified InhA1 from *B. anthracis* A35 NprB- cells. InhA1 consists of a 46 kDa and an 18 kDa polypeptide chains as reported[16].

a)

B. anthracis Ames35

B. anthracis Ames35 ΔInhA1

InhA1 | aggregated | suspended | aggregated

kDa
100 –
75 –   ◄ InhA1 75 kDa
50 –
37 –   ◄ InhA1 46 kDa
25 –
20 –

b)

	Ratio of InhA1 produced in aggregated / suspended cultures (± SE)
InhA1 75 kDa	0.82 ± 0.08
InhA1 46 kDa	0.88 ± 0.11

Figure S8. Comparison of InhA1 production in aggregated versus suspended cultures of *B. anthracis* Ames35. (a) Immunoblot of InhA1 expression from *B. anthracis* Ames35. Purified InhA1 (10 µg) in lane 1 was used to determine the presence of two forms of InhA1 – InhA1 75 kDa and InhA1 46 kDa – in the supernatant of both clustered (aggregated) and dispersed (suspended) Ames35 cultures. The InhA1 deficient Ames35 ΔInhA1 mutant was used as a negative control. Plate cultures for this immunoblot were grown at 37° C overnight and incubated in PBS for 1 hour, the same growth conditions used in bacterial coagulation experiments. Samples shown are after TCA precipitation. (b) Ratio of InhA1 produced from aggregated vs. suspended *B. anthracis* A35. Results based on three independent experiments.
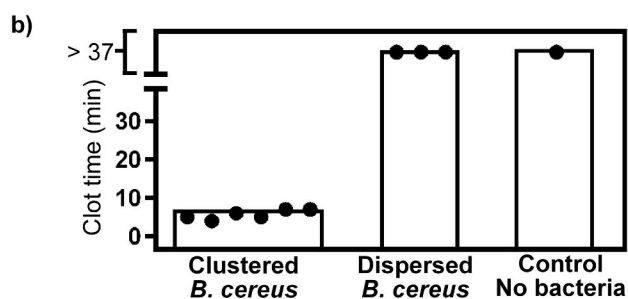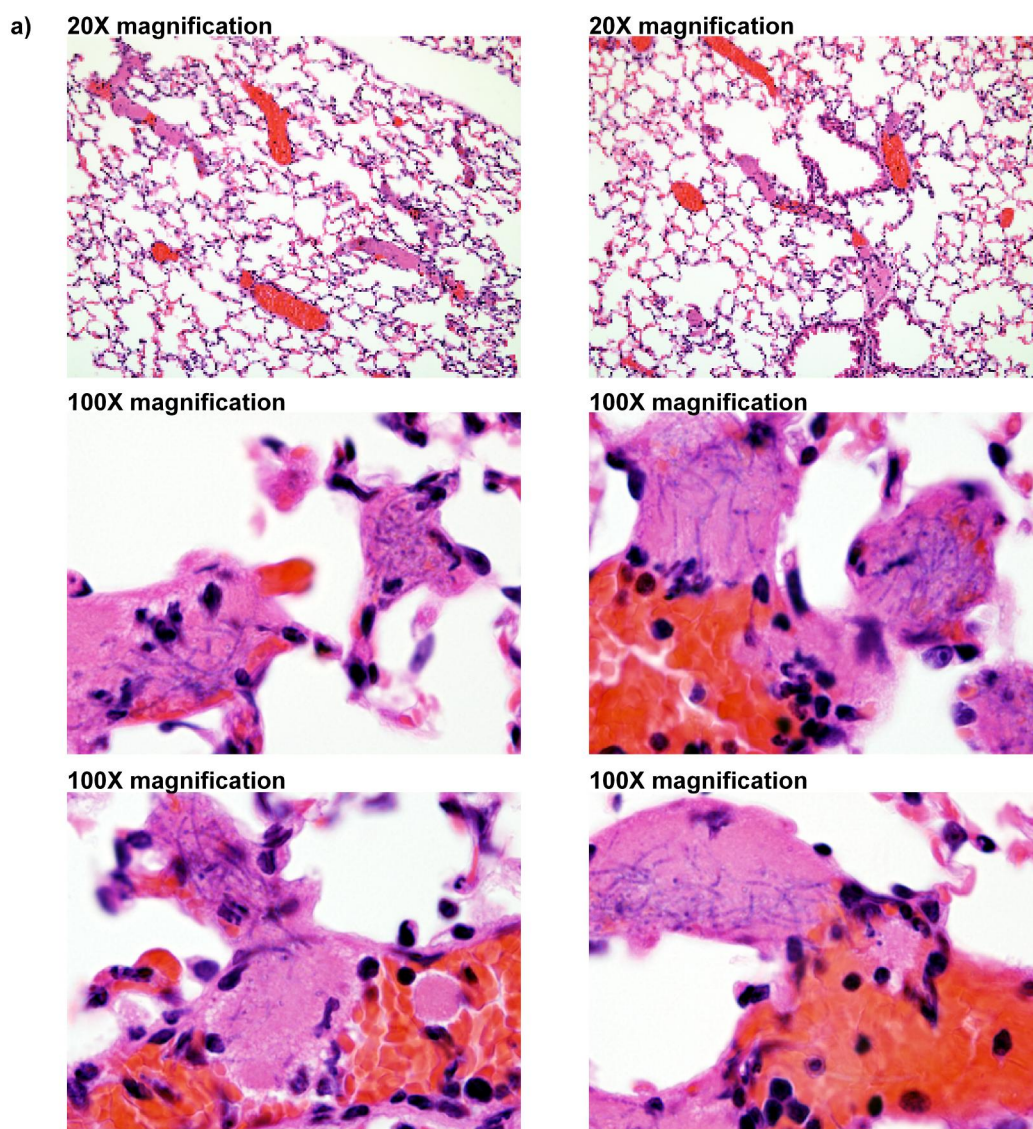
Figure S9. Coagulation of mouse blood and plasma on clusters of bacteria, *in vivo* and *in vitro*. (a) Additional images of coagulation on clusters of *B. anthracis* in mice. These images were taken during the experiment that is described in Fig. 6 of the main text. (b) *In vitro*, mouse blood plasma coagulated rapidly by *B. cereus* (ATCC #14579) when the bacteria were spatially localized, but not when the bacteria were dispersed in solution. Clot times of mouse blood plasma in a microfluidic chamber were measured using fluorescence microscopy. The plasma was exposed to the same amount of bacteria either clustered in a large patch or dispersed in solution.

SUPPLEMENTARY METHODS

Bacterial strains

Bacillus cereus (*B. cereus*) GFP was *B. cereus* UW85 43-25 (source, J. Handelsman)[1]. *Escherichia coli* (*E. coli*) Ymel-1 is a K-12 mutant strain that is deficient in Curli, an amyloid surface protein (source H. Herwald)[2]. *E. coli* Ymel-1 GFP was prepared by transformation with pUCP24/EGFP plasmid by using electroporation. The *B. cereus* strain used in Fig. 1b, 3, 4, and S1-S5 (*B. cereus* L. I.) was a wild-type strain and its identity was confirmed by sequence alignment of the clpC and dinB genes with sequences in GenBank (preformed by Genewiz, Inc., SouthPlainfield, NJ). The following strains were obtained from the American Type Culture Collection (ATCC): *B. cereus* ATCC#14579, *B. thuringiensis* ATCC#35646, *B. licheniformis* ATCC#25972, *B. subtilis* ATCC#6051, *B. circulans* ATCC#4513, and *S. aureus* ATCC#25923. All *B. anthracis* strains were non-virulent (pXO1$^+$ pXO2$^-$). The *B. anthracis* strains Δ*nprB* and Δ*inhA1* were Ames 35 0599-LoxP and Ames 35 1295-LoxP, respectively. BA0599 and BA1295 were removed by using Cre recombinase, using a previously described method[3]. This previous work[3] also describes the validation of plasmids used for NprB inactivation along with genotypic consequences and phenotypic effects of the inactivation in *Bacillus anthracis*. The genomic sequence of the Δ*inhA1* strain after inactivation of BA1295 is shown in Fig. S6. The other mutants in the small library of *B. anthracis* Ames 35 strains corresponded to removal of *spo0A*, BA0672, BA1288, BA1290, and BA3159, and these strains were also prepared by using Cre recombinase. The *B. anthracis* 34F$_2$ Δ luxS strain was obtained from M. Blaser[41].

Culturing bacteria

Bacteria were grown on agar plates containing 1% casamino acids (Acros, Fairlawn, NJ), 0.15% yeast extract (Fisher Scientific, Fair Lawn, NJ), 50 μg /mL^{-1} MgSO$_4$, 5 μg/ mL^{-1} MnCl$_2$, and 2% agar (Fisher Scientific, Fair Lawn, NJ) at 25° C for 14---24 hrs. The coagulation phenotype of *B. anthracis* was not specific to this growth condition only, as coagulation also occurred rapidly (< 5 min) and reproducibly (>20 experiments on >5 different days) on *B. anthracis* grown on Luria-Bertani (LB) (Difco, Sparks, MD) plates at 37° C for 14---24 hrs. *B. cereus* encapsulated in GMDs were grown in flowing liquid LB media at 25° C for 14---24 hrs. Antibiotics were used where appropriate.

Preparing bacterial samples

For experiments measuring the initiation of coagulation on clusters of bacteria that were not spatially patterned (Fig. 1b, 3, 4a, 4e, 4f S1, S2 and S9b, but not Fig. 1c and d), bacteria were gently scraped off the plate and suspended in saline at an optical density (O.D. at 600 nm) = 1 in a microcentrifuge tube, which was ~4 × 10^7 cfu/mL for *B. cereus* and ~1 × 10^7 cfu/mL for *B. anthracis*. Bacteria were localized in a pellet at the bottom of the microcentrifuge tube by centrifuging at 11,000 g for 10 min. The supernatant was removed following centrifugation, and ~50 nL droplets of the concentrated bacteria were pipetted onto the plastic coverslip in the bottom of the microfluidic chamber. 100 μL of recalcified plasma was added to the chamber. The bacteria were either dispersed in the plasma by mixing for ~2 s (Fig. 1b and S9b), or the bacteria were allowed to remain localized in a patch (Fig. 1b, 3, 4a, 4e, 4f S1, S2 and S9b). Bacteria remained localized due to weak adhesive forces between themselves and the plastic coverslip.

Micropatterning techniques were used to spatially pattern bacteria (Fig. 1c and d)[4-6] Bacteria were patterned on substrates consisting of alumina membranes (200 nm pore size, Whatman Int. Ltd., England) coated with patterned "positive" photoresist (S1813 Shipley positive tone photoresist, Rohm and Hass, MA). The photoresist was patterned by a photolithography process that selectively opened

the pores of the membrane[6]. Specifically, the membranes were spin-coated with photoresist at 3000 rpm for 10 min, exposed to UV light through a photomask, baked at 125 ºC for 75 sec, and then developed in CD26 for 9 min. The final substrates were rinsed thoroughly with water and heated at 125 ºC for an additional 10 min to inactivate the photoresist layer. The substrates contained arrays of patches of exposed alumina membrane in a background of photoresist. The patterns contained 19 arrays of 60 μm patches as well as single 262 μm patches. To pattern bacteria, a solution of suspended bacteria (O.D. = 1) in saline was placed on top of the substrate, and gentle vacuum was applied from under the substrate to pull the bacteria to the open pores. This step was accomplished by placing the substrate over a hole in a rubber cork attached to a vacuum flask. Excess bacteria were rinsed away with saline while the vacuum was still applied. The patches of bacteria were slightly larger than the patterned patches of the substrate due to a small degree of spreading (~15 μm) of the bacteria when the vacuum was removed. Integrating the fluorescence intensities of the bacteria confirmed that the same amount of bacteria was present in the arrays of patches as in the large single patches.

　　To prepare gel microdroplets (GMDs)[7,8] (Fig. 2), bacteria were first concentrated by centrifugation, and the supernatant was removed. Then, 500 μL of a melted agarose solution was added to the microcentrifuge tube. The agarose solution contained agarose (4%, type IX, Sigma-Aldrich, St. Louis, MO), pluronic F-68 (20 μL of a 10% solution, Sigma-Aldrich, St. Louis, MO), Biomag® amine magnetic particles (1.5 μm diameter, 100 μL of a solution at 50 mg/mL, Bangs Laboratories, Inc., Fishers, IN), and liquid LB growth media (400 μL, Difco LB broth, Miller, Sparks, MD). The agarose solution containing bacteria was separated into droplets ~50 μm in diameter by using a microfluidic approach[9] and cooled to 4° C to solidify the agarose.

　　For experiments testing the activation of purified coagulation factors with whole bacteria cells, (Fig. 4a, 4b, S3 and Fig. S4) the bacteria were suspended in Hepes buffered saline (20 mM Hepes, 150 mM NaCl, 2 mM $CaCl_2$, pH 7.4) at O. D. = 1 at a wavelength of 600 nm. For experiments testing the activation of purified coagulation factors by secreted bacterial components (Figure S5), a solution of suspended bacteria was prepared containing 5 mg of solid bacteria per mL of buffer. This solution was vortexed for 2 min, incubated for 30 min, vortexed for 2 more min, then centrifuged followed by collection of the supernatant.

Measuring clot times of plasma and whole blood
　　This procedure is similar to previously described procedures[10,11]. Citrated human platelet-poor plasma that was pooled from multiple donors was obtained from George King Biomedical, Inc. (Overland Park, KS). Citrated immunodepleted plasmas were obtained from Haematologic Technologies, inc. (Essex Junction, VT), and were accompanied with values for the measured PT and APTT. Human whole blood was obtained from individual healthy donors in accordance with the guidelines set by the Institutional Review Board (protocol # 12502A) at The University of Chicago. Sodium citrate was added to whole blood during the collection to temporarily inhibit the activation of clotting factors. Citrated mouse plasma was obtained by nicking the tail vein and collecting 90 μL blood into10 μL of a sodium citrate solution (32 mg/mL) in a plastic microcentrifuge tube. Mouse plasma was separated from blood by centrifuging twice at 15,000 rpm for 10 min. All blood and plasma samples were incubated with corn trypsin inhibitor (100 μg/mL) to inhibit the factor XII pathway of initiation of coagulation, with the exception of the experiment testing clustered bacteria versus dispersed bacteria with human plasma (all samples in Fig. 1b) and the experiment with immunodepleted plasmas (Fig. 3b and c)[12]. Human plasma was recalcified in 300 μL aliquots by adding 100 μL of a solution of 40 mM $CaCl_2$, 90 mM NaCl and 0.4 mM of a thrombin-sensitive fluorescent substrate, *t*-butyloxycarbonyl-β-benzyl-L-aspartyl-L-prolyl-L-arginine-4-methyl-coumaryl-7-amide (Boc-

Asp(OBzl)-Pro-Arg-MCA) (Peptides International, Louisville, KY). Mouse plasma was recalcified by the same procedure, except in smaller 60 µL aliquots. Clot times were determined by placing recalcified plasma in contact with the bacteria in a microfluidic chamber. The microfluidic chamber consisted of two plastic coverslips (Hampton Research, Aliso Viejo, CA) separated by a silicone isolator (1 × 9 mm, Sigma-Aldrich, St. Louis, MO) coated with an inert fluorinated grease (Krytox, Dupont, Wilmington, DE). The appearance of fibrin was difficult to detect in mouse plasma, although an obvious transition from liquid to gel occurred during clotting on clustered bacteria but not in the control experiment. In addition, some background cleavage of the fluorescent substrate occurred in all mouse plasma samples and this did not correspond to coagulation. Therefore, to identify the burst of thrombin formed during the activation of the coagulation cascade, we took the derivatives of the curves of intensity versus time to obtain the rates of fluorescent substrate cleavage. The clot time in mouse plasma samples was defined as the time when the rate of substrate cleavage was one half of the maximum value observed in the samples that coagulated. For human blood and plasma, when clot times were measured in microfluidic devices whole blood was recalcified in the device by flowing whole blood at a flow rate of 1.6 µL/min and a solution of $CaCl_2$ and Boc-Asp(OBzl)-Pro-Arg-MCA (100 mM $CaCl_2$ and 1 mM Boc-Asp(OBzl)-Pro-Arg-MCA) at a flow rate of 0.2 µL/min[13]. The device contained rectangular cross-section channels. The dimensions of the channels were 100 µm × 100 µm, except in the larger region that contained the GMDs, which extended to 400 µm × 100 µm. The flow profile in this type of geometry has been characterized previously[14]. In the main channel of the device that contained the GMDs, the flow rate was 0.9 µL/min, which corresponds to an average flow velocity of 0.0015 m/s and a shear rate of 140 s^{-1} at the center of the wall for the 100 µm × 100 µm portion of the channel. In all experiments, clot times were determined by monitoring the formation of thrombin and fibrin. The formation of thrombin was monitored by fluorescence microscopy to detect the cleavage products from the thrombin-sensitive fluorescent substrate, Boc-Asp(OBzl)-Pro-Arg-MCA. The formation of fibrin was detected by using brightfield microscopy. The clot time was defined as the first appearance of fibrin, which always correlated with the beginning of increasing fluorescence from thrombin generation.

Statistical analysis

P-values were calculated by the student's t-test. In experiments measuring initiation of coagulation on clusters of bacteria, after human blood plasma was added to the surface cluster of bacteria it took 2-3 min to begin imaging. Coagulation on the surface cluster sometimes occurred prior to the first image at 2-3 min, as indicated by breaks in the Y-axis in the graphs in the figures. When calculating p-values for these samples a conservative clot time value of 2 or 3 min (equal to the delay before imaging in that particular experiment) was used.

Preparing microfluidic devices for measuring clot times of flowing blood and plasma on colonies of bacteria

Measuring coagulation of flowing blood in microfluidic devices has been described previously[14,15] and will be briefly described here. All devices were fabricated by using rapid prototyping in PDMS. The devices were sealed by using a Plasma Prep II (SPI Supplies, West Chester, PA) and baked overnight at 110 ºC. The devices were then placed into a saline solution and kept under vacuum overnight to completely saturate the PDMS. Solutions were flowed into the microfluidic devices through FEP tubing (1/32 inch outer diameter, Upchurch Scientific, Oak Harbor, WA) connected to glass or plastic syringes. For handling blood, the tubing was connected to plastic syringes (1 mL, Becton Dickson, Franklin Lakes, NJ) and the syringes were blocked with a solution containing Pluronic F127 surfactant prill (0.2% in phosphate buffered saline, BASF, Mt. Olive, NJ). Prior to adding the

GMDs or blood, microfluidic channels were coated with inert phospholipids by flowing vesicles of L-α-phosphatidylcholine (1.25 mg mL^{-1}, egg yolk derived, Avanti Polar Lipids, Alabaster, AL) through the device at a flow rate of 1.0 μL min^{-1} for 20 min. Excess vesicles were removed from the channels by flowing a solution of saline through them for 10 min at 1.0 μL min^{-1}. GMDs containing bacteria were flowed into the device and localized near the magnets. Bacterial colonies were grown from the GMDs in the microfluidic device by flowing LB broth over them for 14-24 h. After bacterial colonies were present, whole blood was flowed through the device as described above. The formation of thrombin and fibrin was monitored throughout the device during the experiment.

Analysis of fluorescence images

Image analysis was preformed as previously described[10]. The original grayscale fluorescence images were collected and false-colored by using MetaMorph software (Molecular Devices, Sunnyvale, CA). For each wavelength, the levels were adjusted to the same values. Images were overlaid by using adobe Photoshop software (Adobe, San Jose, CA).

Purifying InhA1

InhA1 was purified from the *B. anthracis* ΔAmes 35 (pXO1$^+$, pXO2$^-$, NprB$^-$) strain (**Fig. S7**). After overnight culture in LB medium at 37°C, the culture supernatant was collected by centrifugation and concentrated by 75% ammonium sulfate precipitation. InhA1 was purified by using two sequential chromatographs: a DEAE Trisacryl Plus M anion-exchanger, and a Superdex S-200 size exclusion column (Sigma-Aldrich, St. Louis, MO).

Measuring activation of purified coagulation factors

The activation of coagulation factors was determined by detecting the cleavage of fluorogenic or chromogenic substrates for the activated coagulation factors. For measuring the activation of coagulation factors by whole cells or purified InhA1, fluorescence measurements were taken, and for measuring the activation of coagulation factors by secreted components from cells, absorbance measurements were taken. Fluorescence measurements were taken by using a Tecan Safire 2 microplate reader. 100 μL of a solution of *B. anthracis* cells (O.D. at 600 nm = 1, ~1×10^7 cfu/mL) or purified InhA1 (0.2 mg/mL) mixture was placed in wells in micro-plates. Prothrombin or factor X were then added to the wells at concentrations[17] of 1400 nM, and 160 nM, respectively. Coagulation factors were purchased from Haematologic Technologies, Essex Junction, VT. Fluorogenic substrates (1 μL of 1 mM solution containing 10% dimethyl sulfoxide in HBS buffer) corresponding to the activated coagulation factor were then added to the wells, and changes in fluorescence intensity were measured. Fluorogenic substrate Boc-Asp(OBzl)-Pro-Arg-MCA (Peptides International, Louisville, KY) was used to detect thrombin, and Z-Pyr-Gly-Arg-MCA (Peptides International, Louisville, KY) was used to detect factor Xa[18]. Absorbance measurements were taken using a BMG Labtech POLARstar Omega microplate reader. 100μL of the secretion solution was placed in wells in micro-plates and the purified coagulation factor was added to a final a concentration of 100 nM. The corresponding chromogenic agent was added to the wells to a final concentration of 50 μM, and the change in absorbance was measured. Spectrozyme chromogenic substrates specific for each coagulation factor were purchased from American Diagnostia, Stamford, CT. The curves shown in Fig. S5 indicate the absorbance values after the curves from two control experiments, i) without secreted components and ii) without the coagulation factor, were subtracted.

Measuring the production of InhA1 from clustered versus dispersed B. anthracis

13

Bacterial lawn cultures of *B. anthracis* Ames 35 strain and InhA deletion mutant ΔInhA1 were grown on LB plates at 37° C overnight and either used right away or kept at room temperature for an additional 24 hours. The bacteria were gently scraped off the plates and washed twice with sterile PBS. Cells were resuspended in PBS to OD600 = 1. To mimic the clustered state, *B. anthracis* Ames 35 wild type and ΔInhA1 cultures were pelleted. To mimic the dispersed state, an equal volume of *B. anthracis* Ames 35 culture underwent constant shaking at 65-70 rpm. Cultures for both conditions were incubated at 37° C for 1-2 hours. After incubation, supernatant from all cultures was filtered and concentrated to 1 ml. Equal volumes of concentrated supernatant, either with or without trichloroacetic acid (TCA) precipitation, were run on 13% SDS-PAGE, and immunoblot analysis was performed using mouse anti-InhA1 serum (kindly provided by Drs. Patricia Sylvestre and Michèle Mock at the Pasteur Institute in Paris) and goat anti-mouse IRDye fluorescent secondary antibody (Licor Biosciences, Lincoln, NB). Immunoblot band intensity was measured using the Odyssey Infrared Imaging System and software (Licor Biosciences, Lincoln, NB).

Numerically simulating initiation of coagulation by bacteria

Numerical simulations were performed by using a commercial finite element package (Comsol Multiphysics 3.3, Comsol, Stockholm, Sweden) and a reaction kinetics package (Comsol Reaction Engineering Lab, 1.2). In total 40 rate equations and 45 species of the coagulation network were incorporated in the simulation. For the reactions of the coagulation cascade, all reactions, rate constants, and initial concentrations used were identical to a well established model[19], with the addition of the activation of factor X to factor Xa by factor IXa[20], and the inhibitions of factor IIa and factor Xa by α_1-antitrypsin and the inhibition of factor IIa by α_2-macroglobulin[21]. When the three additional inhibition reactions were not included, the model reproduced published results[19]. Inclusion of the inhibition reactions had the effect of lengthening the initiation phase of clotting. For example, when initiation occurred with 5 pM of tissue factor, the peak thrombin concentration (0.33 μM, total thrombin and meizothrombin) was reached at 14.4 min for the modified model, instead of 11.7 min for the original model. The inclusion of these inhibition reactions should also increase the threshold patch size, which is the critical size of a patch of stimulus required to initiate clotting[10,11]. In this simplified simulation, the presence of bacteria was represented by a concentration of bacterial surface catalyst that activated prothrombin and factor X. The effect of bacteria on activation of coagulation reactions was introduced into the model by including two extra second-order reactions, II + Bac → IIa + Bac and X + Bac → Xa + Bac, with rate equations $R_{IIa} = k_{IIa}$ [Bac] [II] and $R_{Xa} = k_{Xa}$ [Bac] [X], respectively, where [Bac] represents the unitless concentration of bacteria. The rate constants for activation of prothrombin and factor X by bacteria were determined experimentally in kinetic assays assuming Michaelis Menton kinetics for cleavage of fluorogenic substrates, Boc-Asp(OBzl)-Pro-Arg-MCA by prothrombin, and Z-Pyr-Gly-Arg-MCA by factor X. The calculated rates of activation of prothrombin (1.4 μM) and factor X (160 nM) were 1.6×10^{-21} and 7.4×10^{-22} M s^{-1} per bacterium, respectively. A diffusion coefficient of 5×10^{-11} m^2/s was used for all species except for bacteria, fibrin, TF, and all complexes with TF, for which the diffusion coefficient was zero[22]. In discussions of the simulation, thrombin concentration is reported as the total concentration of both thrombin and meizothrombin, as in previous experiments[19].

Measuring coagulation by B. anthracis in mice

All animal experiments and protocols were approved by and conducted according to the guidelines of the NIAID Animal Care and Use Committee. Solutions containing *B. anthracis* (vegetative cells) were grown overnight on LB agar and suspended directly from plates in phosphate buffered saline (PBS) at a concentration of either 10^5 or 10^9 CFU /mL^{-1}. 100 μL of the bacteria solution

waswere injected intravenously (IV) into the tail vein of DBA/2J mice (Jackson Laboratories). After 30 or 90 min, organs were harvested and immediately fixed in a neutral-buffered 10% formalin for Hematoxylin and Eosin (H&E) staining.

Confirming that coagulation was initiated by activation of the coagulation network

To test whether coagulation occurred by cleavage of fibrinogen alone or by activation of other coagulation factors and the coagulation network, we performed the "coagulase" assay (**Fig. S1**). This assay is commonly used to test for "coagulase" enzymes that activate fibrinogen in the absence of Ca^{2+}. Ca^{2+} is required for activation of most coagulation factors, such as prothrombin. Coagulase activity was measured by using the CoaguStaph kit (Hardy Diagnostics, Santa Maria, CA) which contains rabbit plasma and EDTA. The procedure provided with this kit was followed.

When rabbit plasma containing EDTA was exposed to the control "coagulase positive" strain, *S. aureus*, coagulation occurred within 1 h. However, when the plasma was exposed to *B. cereus* or *B. anthracis*, coagulation did not occur within 26 h. This result confirms that initiation of coagulation by *B. cereus* and *B. anthracis* does not involve traditional "coagulase" enzymes.

Additional control experiments also demonstrated that initiation of coagulation by *Bacillus* species involved activation of the coagulation cascade. The coagulation response by *Bacillus* species does not occur in the absence of Ca^{2+}, which is required for activation of coagulation factors. Coagulation still occurs in the experiments when the MCA substrate is not present, as seen by fibrin formation by using brightfield microscopy.

Testing initiation of coagulation of von Willebrand disease plasma by bacteria.

Recent experiments have shown that InhA1 from *B. anthracis* can cleave von Willebrand factor, a regulator of platelet aggregation[16]. To test whether von Willebrand factor was required for initiation of coagulation of plasma by *B. cereus* and *B. anthracis*, we used platelet poor plasma from a donor with severe trait von Willebrand disease (vWD) (**Fig. S2**). According to the supplier (George King Biomedical, Inc), the concentration of von Willebrand factor in vWD plasma was 3% of the concentration of von Willebrand factor in normal pooled plasma (NPP) from healthy donors. The activity of coagulation factor VIII in vWD plasma was 5% of the activity of factor VIII activity in NPP. *B. cereus* and *B. anthracis* still rapidly initiate coagulation of plasma deficient in von Willebrand factor and platelets, with clot times of 2-6 min. These clot times are comparable to the clot times of 2-5 min for NPP. For comparison, we tested the clot time of plasma depleted in prothrombin, and found this clot time to be longer than 30 min. The slightly longer clot times of vWD plasma compared to NPP are likely due the reduced factor VIII activity [23]. Additionally, we observed that clots of vWD plasma spread (propagated) slowly after initiation by the bacteria, which is also consistent with reduced factor VIII activity [23].

Measuring the production of InhA1 from clustered versus dispersed B. anthracis

To test whether clustering B. anthracis lead to increased production of InhA1 we performed an immunoblot experiment using mouse anti-InhA1 serum (**Fig. S8**). Clustered (aggregated) and dispersed (suspended) bacteria produced very similar amounts of InhA1, with aggregated cultures producing slightly less. This experiment ruled out the hypothesis that the clustering of bacteria lead to increased production of InhA1 which then triggered coagulation, and supports the hypothesis that spatial localization controls initiation of coagulation by bacteria.

SUPPLEMENTARY REFERENCES

1. Dunn, A.K. & Handelsman, J. A vector for promoter trapping in Bacillus cereus. *Gene* **226**, 297-305 (1999).
2. Herwald, H. et al. Activation of the contact-phase system on bacterial surfaces - a clue to serious complications in infectious diseases. *Nat. Med.* **4**, 298-302 (1998).
3. Pomerantsev, A.P., Sitaraman, R., Galloway, C.R., Kivovich, V. & Leppla, S.H. Genome engineering in Bacillus anthracis using Cre recombinase. *Infect. Immun.* **74**, 682-693 (2006).
4. Weibel, D.B., DiLuzio, W.R. & Whitesides, G.M. Microfabrication meets microbiology. *Nat. Rev. Microbiol.* **5**, 209-218 (2007).
5. Whitesides, G.M., Ostuni, E., Takayama, S., Jiang, X.Y. & Ingber, D.E. Soft lithography in biology and biochemistry. *Annu. Rev. Biomed. Eng.* **3**, 335-373 (2001).
6. Li, F., Zhu, M., Liu, C.G., Zhou, W.L. & Wiley, J.B. Patterned metal nanowire arrays from photolithographically-modified templates. *J. Am. Chem. Soc.* **128**, 13342-13343 (2006).
7. Weaver, J.C., Williams, G.B., Klibanov, A. & Demain, A.L. Gel Microdroplets - Rapid Detection and Enumeration of Individual Microorganisms by Their Metabolic-Activity. *Bio-Technology* **6**, 1084-1089 (1988).
8. Zengler, K. et al. Cultivating the uncultured. *Proc. Natl. Acad. Sci. U. S. A.* **99**, 15681-15686 (2002).
9. Zhang, H. et al. Microfluidic production of biopolymer microcapsules with controlled morphology. *J. Am. Chem. Soc.* **128**, 12205-12210 (2006).
10. Kastrup, C.J., Runyon, M.K., Shen, F. & Ismagilov, R.F. Modular chemical mechanism predicts spatiotemporal dynamics of initiation in the complex network of hemostasis. *Proc. Natl. Acad. Sci. U. S. A.* **103**, 15747-15752 (2006).
11. Kastrup, C.J., Shen, F., Runyon, M.K. & Ismagilov, R.F. Characterization of the threshold response of initiation of blood clotting to stimulus patch size. *Biophys. J.* **93**, 2969-2977 (2007).
12. Lo, K. & Diamond, S.L. Blood coagulation kinetics: high throughput method for real-time reaction monitoring. *Thromb. Haemost.* **92**, 874-882 (2004).
13. Rivard, G.E. et al. Evaluation of the profile of thrombin generation during the process of whole blood clotting as assessed by thrombelastography. *J. Thromb. Haemost.* **3**, 2039-2043 (2005).
14. Runyon, M.K., Johnson-Kerner, B.L., Kastrup, C.J., Van Ha, T.G. & Ismagilov, R.F. Propagation of blood clotting in the complex biochemical network of hemostasis is described by a simple mechanism. *J. Am. Chem. Soc.* **129**, 7014-+ (2007).
15. Song, H. & Ismagilov, R.F. Millisecond kinetics on a microfluidic chip using nanoliters of reagents. *J. Am. Chem. Soc.* **125**, 14613-14619 (2003).
16. Chung, M.C. et al. Degradation of Circulating von Willebrand Factor and Its Regulator ADAMTS13 IMplicates Secreted Bacillus anthracis Metalloproteases in Anthrax Consumptive Coagulopathy. *J. Biol. Chem.* **283**, 95319542 (2008).
17. vantVeer, C. & Mann, K.G. Regulation of tissue factor initiated thrombin generation by the stoichiometric inhibitors tissue factor pathway inhibitor, antithrombin-III, and heparin cofactor-II. *J. Biol. Chem.* **272**, 4367-4377 (1997).
18. Kawabata, S.I. et al. Highly Sensitive Peptide-4-Methylcoumaryl-7-Amide Substrates for Blood-Clotting Proteases and Trypsin. *European Journal of Biochemistry* **172**, 17-25 (1988).
19. Hockin, M.F., Jones, K.C., Everse, S.J. & Mann, K.G. A model for the stoichiometric regulation of blood coagulation. *J. Biol. Chem.* **277**, 18322-18333 (2002).

20. Butenas, S., Orfeo, T., Gissel, M.T., Brummel, K.E. & Mann, K.G. The significance of circulating factor IXa in blood. *J. Biol. Chem.* **279**, 22875-22882 (2004).
21. Kogan, A.E., Kardakov, D.V. & Khanin, M.A. Analysis of the activated partial thromboplastin time test using mathematical modeling. *Thromb. Res.* **101**, 299-310 (2001).
22. Krasotkina, Y.V., Sinauridze, E.I. & Ataullakhanov, F.I. Spatiotemporal dynamics of fibrin formation and spreading of active thrombin entering non-recalcified plasma by diffusion. *Biochim. Biophys. Acta-Gen. Subj.* **1474**, 337-345 (2000).
23. Mann, K.G., Brummel, K. & Butenas, S. What is all that thrombin for? *J. Thromb. Haemost.* **1**, 1504-1514 (2003).